


Cite this: *RSC Adv.*, 2018, 8, 31783

Lubrication and plasticization behavior of large-size micro-spherical structured SiO₂ for natural rubber

Shuai Zhao,* Xiaoming Shao, Xiaolin Liu, Licong Jiang, Zheng Zhao, Shicheng Xie, Lin Li * and Zhenxiang Xin

In many rubber dynamic applications such as tires and seals, imparting excellent flex fatigue properties and processing behavior are of prime importance. Research in this direction has been done based on a judicious choice of polymer type or a blend thereof and the compounding ingredients. In this study, the effect of micro-spherical SiO₂ on the flex fatigue properties and processing behavior of natural rubber (NR) is studied. Two different particle sizes of spherical SiO₂ (N90, average diameter: 200 nm and N98, average diameter: 120 nm) were used to optimize the flex fatigue properties and processing behavior, and the mechanism is investigated. In this blend, 5 phr loading of N90 was effective in imparting the best overall combination of properties. This work was aimed at providing some theoretical basis and application basis for the use of micro-spherical SiO₂ in the rubber industry.

Received 10th July 2018
Accepted 29th August 2018
DOI: 10.1039/c8ra05875j
rsc.li/rsc-advances

1. Introduction

Rubber is one of the most versatile materials having myriad applications—from niche rubber bands to highly engineered spacecraft seals, including products such as tires, innertubes, footwear, conveyor belts, medical devices, bumpers, and numerous other products.^{1–5} Rubber formulations and compounding is the complex technology of selecting and blending the optimum combination of elastomer and other ingredients that meet the performance, processing, environmental, and cost requirements for rubber goods made and used in commerce.^{6–9} Plasticizer is necessary in rubber formulations for improving the processing of the rubber by lowering the compound's viscosity, and also for aiding in low temperature flexibility of the formulated rubber.^{10,11} Aromatic oils predominated as the plasticizers and good process aids in the rubber industry for many years, however, their carcinogenic effect due to the presence within them of polycyclic aromatic hydrocarbons is fatal.¹² Concern about toxicity of highly aromatic oil led to the usage of a nontoxic type of extender oil. These nontoxic oils are mostly distillate aromatic extract (DAE),¹³ treated distillate aromatic extract (TDAE),¹⁴ and mild extraction solvates (MESS),¹⁵ residual aromatic extract (RAE),^{16,17} hydrogenated naphthenic oils (HNAP),^{17,18} naphthenic oils,¹⁶ paraffinic oils^{19–22} which growing as leading plasticizers to instead of aromatic oils. The advantage of these oils is that it is a powerful plasticizer in easing the compounding process of

rubber. However, because of the diffusion of the low-molecular-weight oily plasticizers in the rubber matrix, these oil-plasticized rubber compounds are subjected to the oozing of oil to the rubber surface and the evaporation of oil at elevated temperatures, leading to the decrease of the mechanical properties over time, especially for stiffness and flex fatigue property.^{23–26} What is worse, they often migrate or volatilize from polymer matrix due to the low-molecular-weight leading to serious environmental pollutions.²⁵ Then much attention has been focused on the research of polymeric plasticizers in recent years.^{27,28} The miscibility of the polymeric plasticizers and rubber composite is important for maintaining the physical properties during the thermal aging process. However, their plasticizing effect is limited due to high-molecular-weight compared with oily plasticizers.

A new plasticizer simultaneously with good plasticizing effect and good performance especially in flex fatigue property is a potential candidate that can replace the conventional process oils and polymeric plasticizers. Jiji Abraham *et al.* have studied the effect of different particle size on reinforcing of natural rubber.^{29,30} In the present work, the effects of micro-spherical SiO₂ on the mechanical and processing behaviors of NR have been experimentally investigated. Two different particle sizes of micro-spherical SiO₂ (N90 and N98) were used to optimize flex fatigue property and processing behavior, and the mechanism is investigated.

2. Experimental section

2.1 Materials

N90 (96% SiO₂, average diameter: 200 nm) and N98 (98% SiO₂, average diameter: 120 nm) were supplied by Qingdao Taiyang

Key Laboratory of Rubber-Plastics, Ministry of Education, Shandong Provincial Key Laboratory of Rubber-Plastics, School of Polymer Science and Engineering, Qingdao University of Science and Technology, Qingdao 266042, China. E-mail: lyzhsh@163.com; qustlilin@hotmail.com



Table 1 Batch compositions, in (phr)^a

Items	Amount (phr)						
	1#	2#	3#	4#	5#	6#	7#
NR	100	100	100	100	100	100	100
ZnO	5	5	5	5	5	5	5
Stearic acid	2	2	2	2	2	2	2
N90	0	5	10	15	0	0	0
N98	0	0	0	0	5	10	15
MB	1	1	1	1	1	1	1
2246	1	1	1	1	1	1	1
N330	40	40	40	40	40	40	40
CZ	1	1	1	1	1	1	1
DM	0.6	0.6	0.6	0.6	0.6	0.6	0.6
Sulphur	2.5	2.5	2.5	2.5	2.5	2.5	2.5

^a phr is parts per hundred rubber.

Sheng Chemical co. LTD (China). NR (SVR3L, polyisoprene content is 94%) was provided by Sanlux Co., Ltd (China). Zinc oxide, stearic acid, sulfur, 2-benzimidazolinethione (MB), 2,2'-

methylenabis(4-methyl-6-*tert*-butylphenol) (2246), 2-benzothiazolyl disulfide (DM), *N*-cyclohexyl-2-benzothiazole sulfenamide (CZ) and carbon black (N330) were provided by Sanlux Co., Ltd (China) and industrial grade.

2.2 Preparation of the batches

Mixing was performed in a 200 ml Banbury mixer at a rotor speed of 60 rpm for the mixing stage at a temperature of 80 °C. The NR was fed into the mixer and premixed for 2 min. This was followed by the sequential addition of zinc oxide (5 phr), stearic acid (2 phr), CZ (1 phr), DM (0.6 phr), MB (1 phr) and 2246 (1 phr) mixing the compounding ingredients for another 4 min. Next, N90 or N98 (at a changed ratio) was added followed by N330 (40 phr) and compounded into the rubber for 4 min and then the mixture was discharged onto a two roll mill at 60 °C, where the sulfur (2.5 phr) was added. The batch compositions are shown in Table 1. The batches (2#, 3# and 4#) deal with effects of change in the loading of N90 and the batches (5#, 6# and 7#) deal with effects of change in the loading of N98 at a fixed formula.

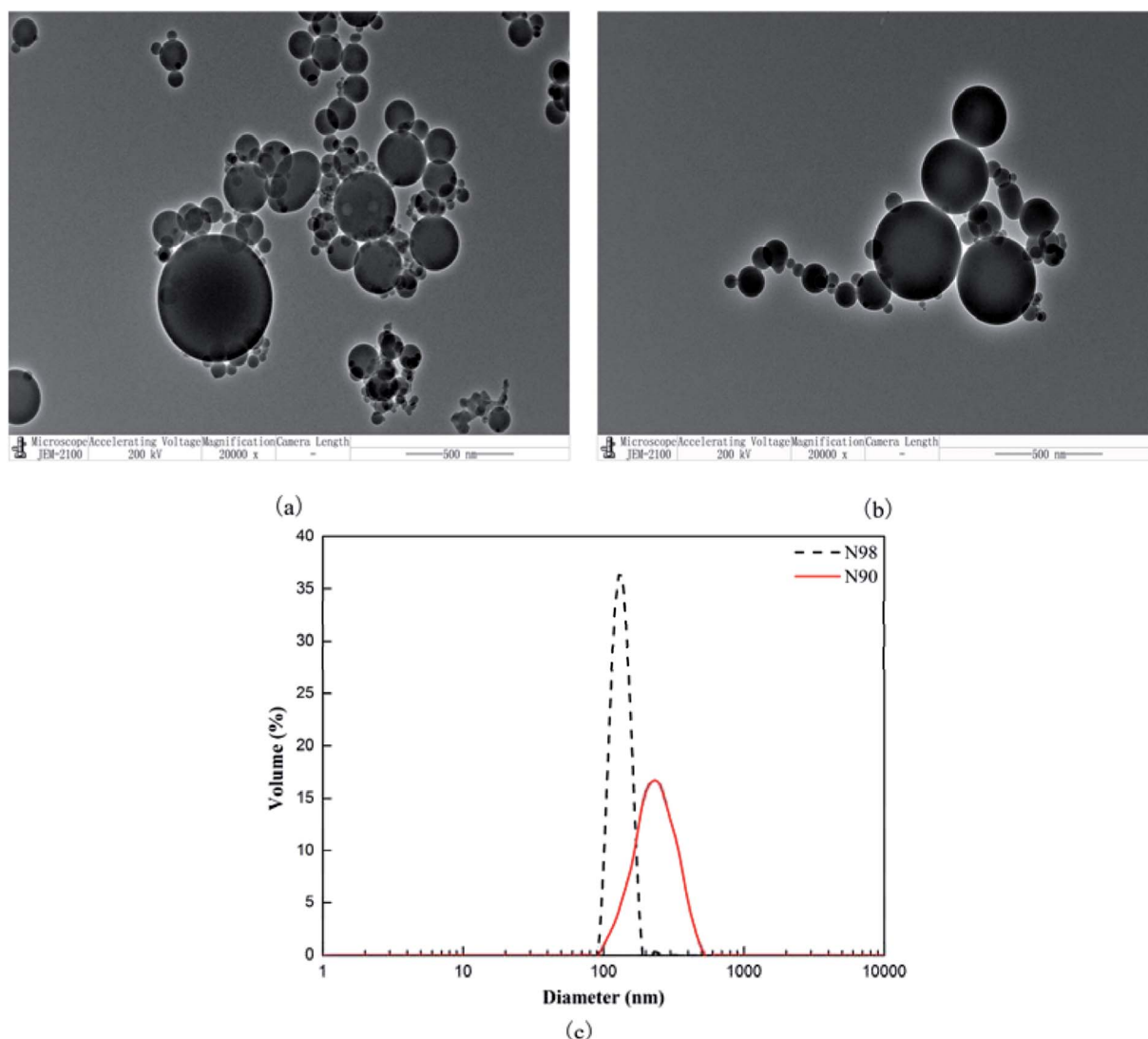


Fig. 1 TEM images of N90 (a) and N98 (b); particle size distribution map of N90 and N98 (c).



2.3 Preparation of test specimens

Test specimens were die cut from the cured sheets and used for testing after 24 h storage at 23 ± 2 °C of temperature and 50% + 5% of humidity.

2.4 Characterization

Transmission electron microscopy (TEM) images were obtained using a JEM-2100 microscope. Scanning electron microscopy (SEM) was performed with JEOL-JSM-7500F microscopy. The infrared spectra were obtained with a Bruker Vertex 70 variable temperature Fourier Transform Infrared Spectrometer. Particle size analysis was measured on a Malvern Zetasizer Nano-ZS system equipped with a 632.8 nm He-Ne laser. Dynamic rheological tests were used to measure the dynamic viscoelastic properties of rubber compounds by Rubber Processing Analyzer (RPA 2000, Alpha Technologies) with strain sweeps performed from 0.25% to 125% at a frequency of 1 Hz and at a temperature of 333 K. Tensile and tear testing were carried out using an AI-7000S Universal Material Tester, with a dumbbell specimen at a tensile speed of 500 mm min⁻¹ according to ISO 528:2009. The cure behavior of the compounds was determined using a Monsanto Oscillating Disc Rheometer (Model XLB-D(Q)350, Hubei, China) at 150 °C. Mooney viscosity (ML_{1+4}^{100} °C) was carried out using an EKT-2000M Mooney viscometer. The dispersity of carbon black was performed on a carbon black dispersion tester (Alpha disperGrader) according to ISO11345. Hardness was reported using the Shore A scale and was measured in a CAS Durometer Type A Model 2001. Flex fatigue property was stretched on a De Mattia Rubber Flexometer (MZ-4003C, Mingzhu, China).

3. Results and discussion

3.1 Morphology of N90 and N98

Both the N90 and N98 particles have amorphous spherical structure as shown in TEM micrographs of Fig. 1a and b. The amorphous micro-scale N90, are severely aggregated with size of 90–400 nm while the morphology of several types of N98 looks alike and their aggregates are much less with size of 90–200 nm as shown in Fig. 1c. The micro-spherical SiO₂ used was of particle form with 96% SiO₂ for N90 and 98% SiO₂ for N98.

3.2 Chemical structure of N90 and N98

From the FTIR spectra of N90 and N98 in Fig. 2, we can see that the stretching vibration peaks of the hydroxyl peaks of silicon hydroxyl, structural water and surface water reach near 3461 cm⁻¹. The symmetric stretching vibration near 810 cm⁻¹, and the anti-symmetric stretching vibration near 1114 cm⁻¹ of Si–O–Si³¹ and bending vibration near 478 cm⁻¹ correspond to Si–O–Si.³² The peak positions of these characteristic peaks are basically consistent with the standard map of SiO₂.

3.3 Morphology of compounds

Fig. 3 represents FE-SEM observations of compounds (1#, 2# and 6#) used for investigating the morphological behavior. In general, the N90 and N98 were found to be uniformly spherical like showing in yellow circles and no obvious structural change was observed for N90 and N98 after tensile failure (Fig. 3b-1 and c-1) in yellow circles. Moreover, it could be clearly observed that N90 and N98 were uniformly dispersed in the matrix. The morphology of carbon black is also recorded to determine how

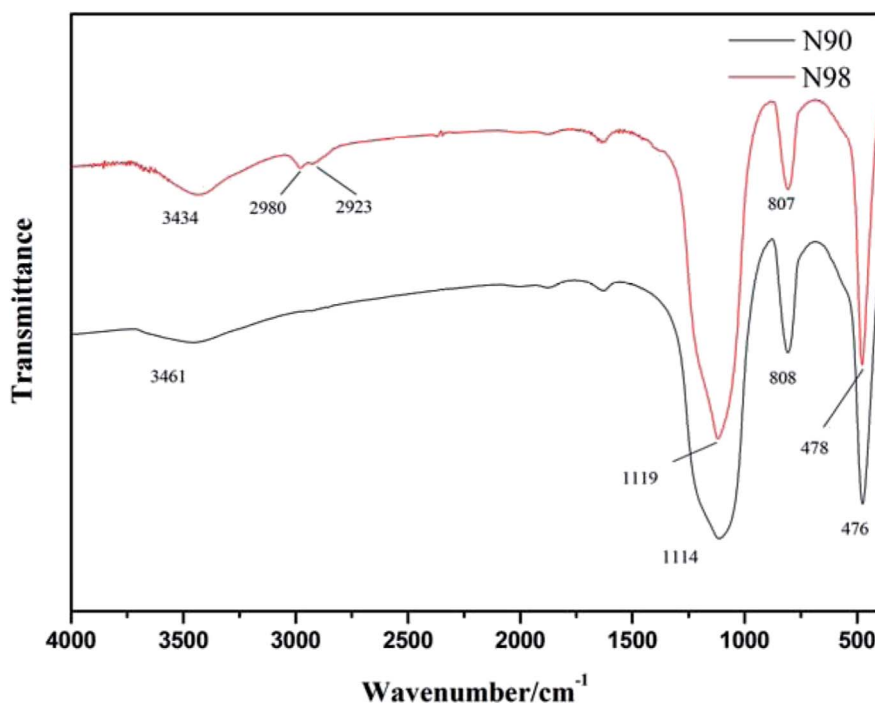


Fig. 2 Infrared spectra of N90 and N98.



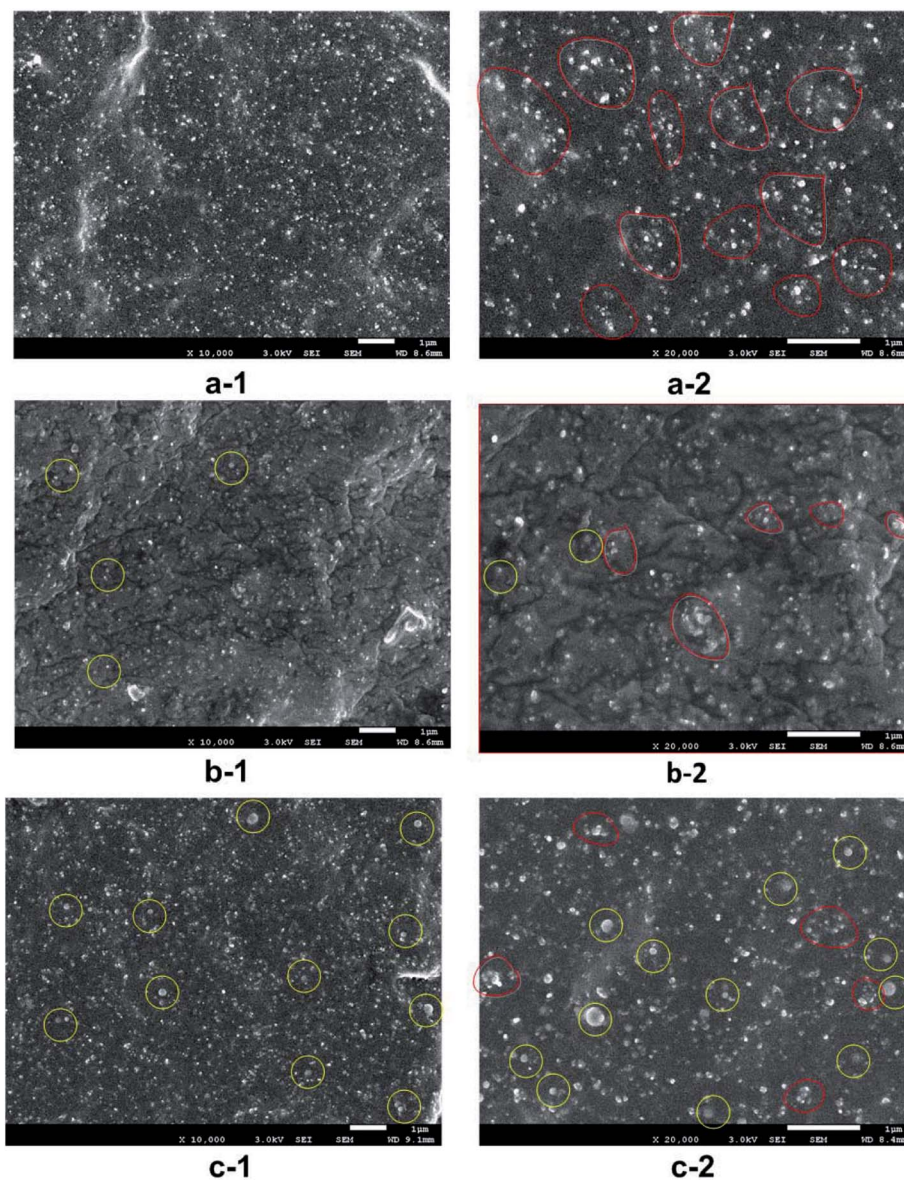


Fig. 3 FE-SEM images of 1# (a-1 and a-2); 2# (b-1 and b-2) and 6# (c-1 and c-2).

is affected by N90 and N98, as shown in Fig. 3. Comparison of the SEM images 'a-1' and 'b-1' in Fig. 3 demonstrates that N90 led to better dispersion of carbon black particles, better compatibility with rubber and reduction of their aggregate size. The good dispersion and reduced aggregation size is especially visible when the magnification is doubled in images 'a-2' and 'b-2' in Fig. 3 outlined in red circles. The same trend is surveyed in Fig. 3c-1 and c-2. The dispersion of carbon black is also certificated by carbon black dispersion photos shown in Fig. 4. As shown in Fig. 4a–d, for NR plasticized with N90 and N98, both the aggregation size and the dispersion of carbon black are obviously improved. It is attributed to boundary lubrication action of spherical N90 and N98 by occupying intermolecular spaces to reduce secondary forces (hydrogen bonding, van der Waals forces...) between carbon black particles.

3.4 Mooney viscosity of compounds

In industrial rubber mixing processes, the Mooney viscosity is a compound measurement of the viscoelastic behavior of an elastomer. It has been widely used for product specification and quality control of non-vulcanized rubbery materials.^{34,35} The Mooney viscosity of the elastomeric compounds is a measure of the flow- and process-ability and is determined by the structure and composition of the rubber. The effect of plasticizer N90 and N98 loading on the Mooney viscosity of the compounds is shown in Fig. 5. It can be seen that for both plasticizers, Mooney viscosity of the compounds is a monotonic decreasing function of N90 and N98 fraction, nevertheless, this relationship changes at higher volume concentrations where increasing N90 and N98 fractions lead to increasing viscosity. The change trend of viscosity with plasticizer loading was similar for both N90 and



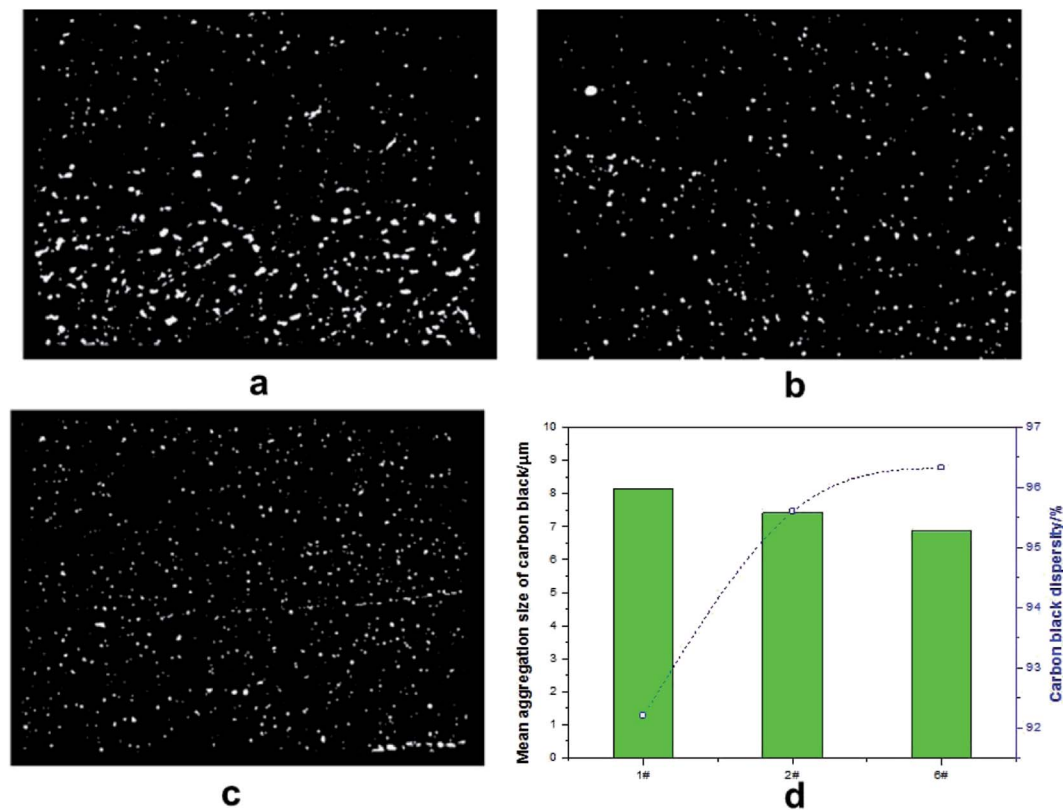


Fig. 4 Carbon black dispersion photos of 1# (a), 2# (b), 6# (c) and mean aggregation size and dispersity of carbon black (d).

N98. The plasticizing effect of N90 and N98 on rubber is also clearly expressed by mixing energy-consume and rubber discharging temperature shown in Fig. 6. These results correspond to the microstructure of NR plasticized with N90 and N98 (Fig. 3 and 4). We attribute that the spherical structure N90 and N98

with lubrication action which reducing the intermolecular frictions and result in lower Mooney viscosities. According to the Hamaker or Lifshitz theory, the van der Waals interaction between particles depends on the geometry of the particle.^{36,37} Thus the shape of sphere would make the van der Waals

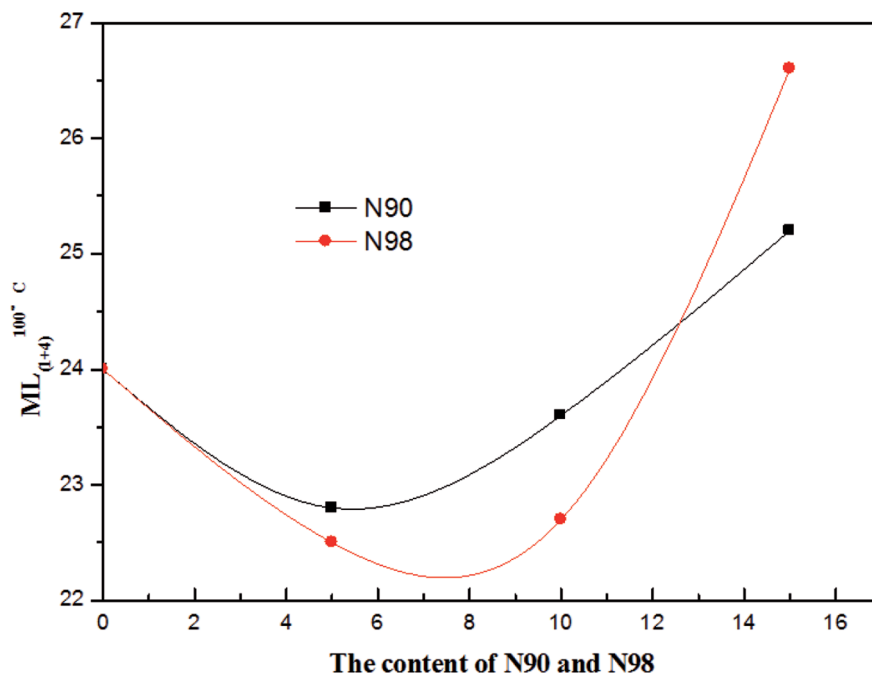


Fig. 5 Mooney viscosity of NR compounds.



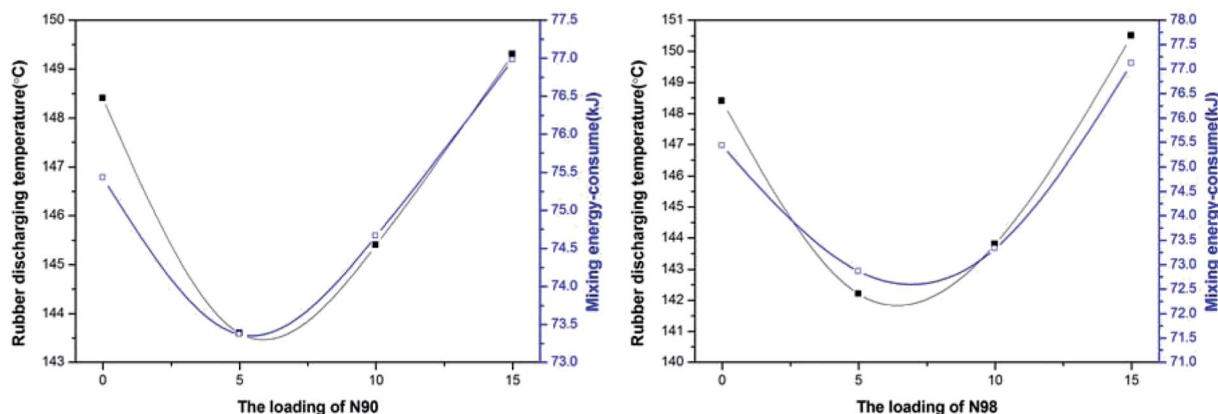
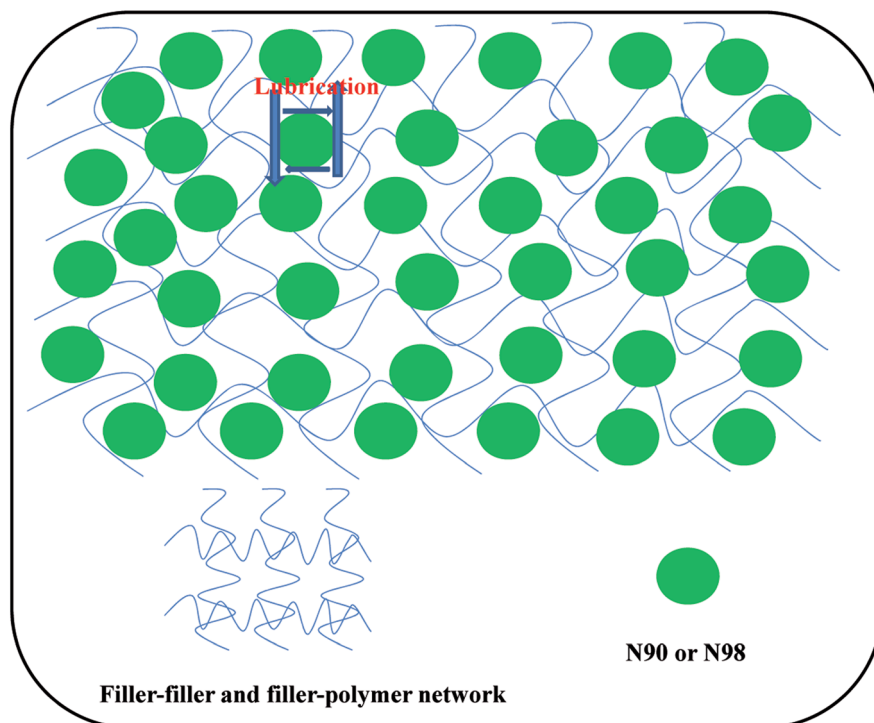


Fig. 6 Rubber discharging temperature and mixing energy-consume of NR compounds with loading N90 and N98 during mixing process.

interaction between N90 and N98 weak. The weak interaction of a spherical plasticizer allows increasing mobility of other fillers such as carbon black and polymer chains by occupying intermolecular spaces and serving as boundary lubricate plasticizers. Thus, these lubricate plasticizers (N90 and N98) insert into fillers and the polymer chains, reducing the intermolecular frictions and decreasing the energy required for molecular motion. The macromolecules slip over each other when spherical plasticizer is rolling when applied load. Then, the spherical plasticizer lubricates the movement of the molecules reducing their internal resistance to slide and to prevent the re-formation of the rigid matrix, as shown in Scheme 1. This efficient slide between molecules can consume a large amount of energy which is responsible for enhanced flex fatigue properties.³³ But

if this lubricating layer consisted of excess plasticizer may induce carbon black and rubber chains complete slippage and the probability for interaction between carbon black particles and rubber chains decreases accordingly at higher volume concentrations of N90 and N98 and lead to failure of lubrication effect of N90 and N98. And that a drop in Mooney viscosity as the spherical plasticizer size increases at a given weight fraction of plasticizer. It is probably because that the molecular number of plasticizer which can occupy intermolecular spaces of carbon black decreases to form an incomplete layer of plasticizer on boundary of carbon black with increasing particle size at a given weight fraction of plasticizer. Therefore, unlike traditional plasticizers, there is effective plasticization for N90 and N98 due to its special lubrication plasticizing mechanism.



Scheme 1 Lubrication theory of spherical SiO₂.



Table 2 Vulcanization behavior of NR compounds^a

Sample	T_{10} (s)	T_{90} (s)
1#	101	444
2#	98	429
3#	99	432
4#	104	412
5#	97	412
6#	104	424
7#	98	439

^a T_{10} and T_{90} are scorch time and cure time, respectively.

3.5 Vulcanization behavior of compounds

The processing safety and vulcanization efficiency of NR compounds plasticized with N90 and N98 expressed in scorch time (T_{10}) and cure time (T_{90}) are depicted in Table 2. The results show that scorch time (T_{10}) of NR compounds nearly keep the same with increasing plasticizers content. Cure time (T_{90}) of NR compounds previously decrease when N90 and N98 content is increased. These results indicate that the processing safety is guaranteed and vulcanization efficiency is effectively improved to increase production efficiency. This is due to lubrication action of N90 and N98 which reducing the inter-molecular frictions and is helpful for the dispersion of

vulcanizing agent and accelerating agent and activating agent. In addition, the gradual decrease in scorch time and cure time when the contents of N90 and N98 are both 5 phr might be because these compounds have experienced greater thermal history during mixing due to this more efficient slide between molecules to consume a large amount of energy under a lower viscosity.³⁸

3.6 Dynamic property of compounds

The influence of N90 and N98 loading on the dynamic viscoelastic behavior of NR compounds can be seen in Fig. 7. After loading the spherical N90 and N98, the low strain modulus rise up a little that resulting in a previous non-linear viscoelastic behavior, known as Payne-effect (Fig. 7a). In all cases the increase of the Payne-effect with different N90 and N98 loading can be still seen. According to the results responded by SEM (Fig. 3), the good dispersion of carbon black should has positive role in Payne-effect, therefore, Payne-effect is caused by filler-filler interactions between carbon black and spherical plasticizer (N90 and N98).³⁹ Fig. 7c gives the corresponding $\tan \delta$ -curves for NR compounds. NR plasticized by N90 and N98 reveals lower $\tan \delta$ in the total strain range. With increasing N90 and N98 loading filler networking develops and stabilizes the viscous polymer fluid yielding a diminished hysteresis behavior at small and intermediate strains. It probability because that

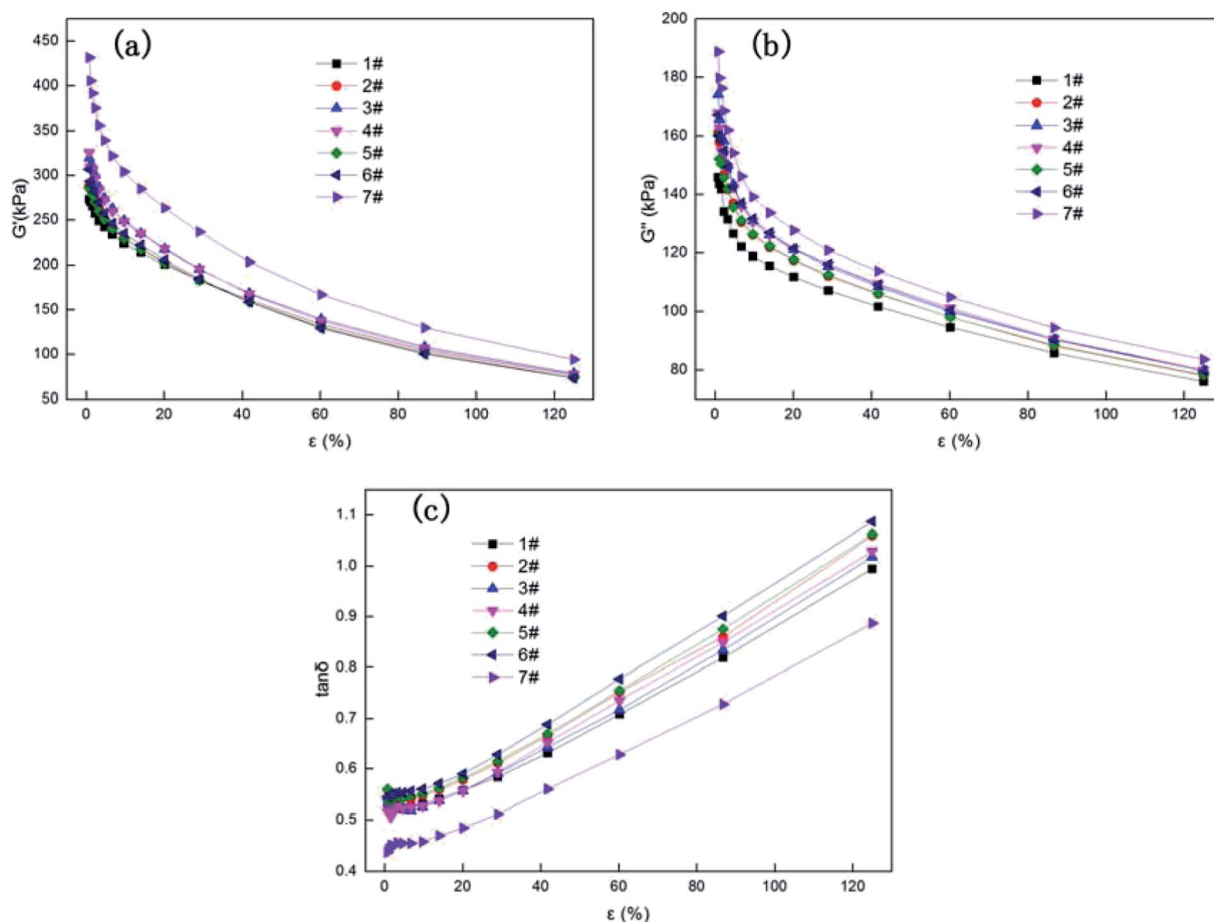


Fig. 7 Viscoelastic behavior of NR compounds: storage modulus- G' (a), loss modulus- G'' (b) and loss factor- $\tan \delta$ (c).



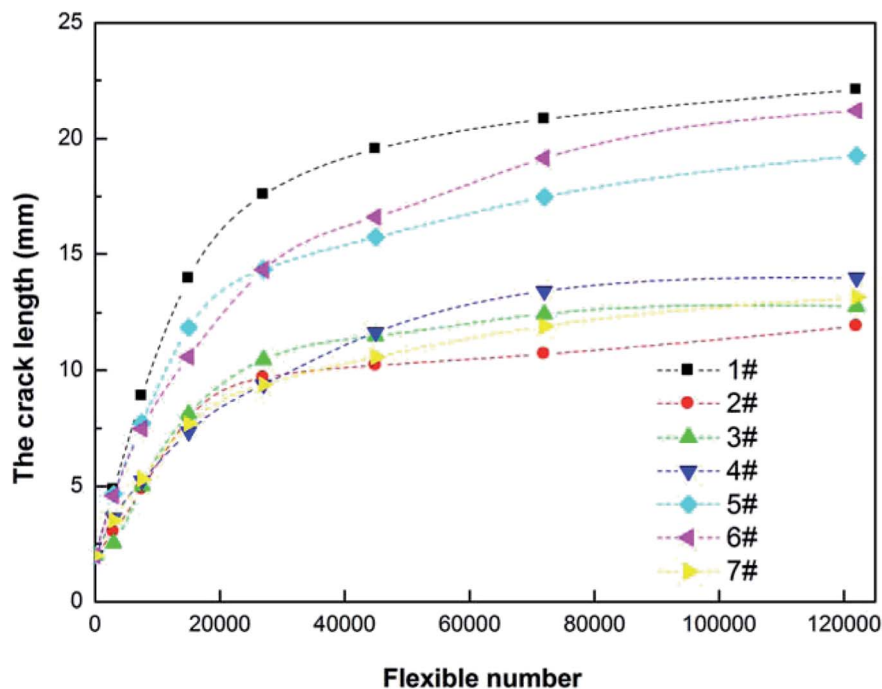


Fig. 8 Flex fatigue properties of NR compounds.

N90 and N98 embedding in rubber chain network play lubrication action and reduce the intermolecular frictions make rubber chains high mobility.

3.7 Flex fatigue property of compounds

It is noteworthy to mention here that while dealing with a plasticized rubber product, the most important properties amongst the properties reported in this work are processing behavior and mechanical property. Usually, the mechanical property of a plasticized rubber is drastically destroyed.^{23–26} Keeping this fact into consideration, the results are analyzed. Flex fatigue property of composites is mainly considered. The dynamic crack growth behavior of NR plasticized with N90 and N98 has been investigated in terms of the incremental changes in crack lengths to the corresponding increases in number of cycles. Then the crack length was plotted with increasing flex cycles shown in Fig. 8. The smallest crack growth rate at a given tearing energy for the NR plasticized with 5 phr N90 denotes the strongest resistance to crack growth compared with the other compounds. It may be attributed to its effective lubricating and plasticizing effect on rubber which rubber chains can adjust conformation in time to obstruct the micro-crack damage and

spread.⁴⁰ It also probably because the compound has experienced greater thermal history during mixing due to this more efficient slide between molecules to consume a large amount of energy.³⁸ When increasing the content of plasticizer, the ability of crack growth resistance decreases, but which is still much better than the neat NR.

These results also correspond to the microstructure of NR compounds characterized by SEM (Fig. 3) and processing techniques denoted in Mooney viscosity (Fig. 5), mixing energy-consume and rubber discharging temperature (Fig. 6).

3.8 Mechanical property

The results obtained for the mechanical properties of the variously compounded samples are presented in Table 3. It is clearly seen from the table that the hardness range is small varying between a minimum of 47 to a maximum of 48 Shore A. It is also seen from the table that the highest tensile strength of 25.02 MPa is with 5 phr N90 followed by 10 phr N98 showing a value of 24.33 MPa. What is more important is to explore tear resistance property. It is seen that tear strength drastically increases with the use of spherical N90 and N98. The maximum tear strength (84.73 Mpa) is obtained using 5 phr N90 compared

Table 3 Mechanical properties of NR compounds

Project	1#	2#	3#	4#	5#	6#	7#
Tensile strength/MPa	25.43	25.02	23.64	21.87	22.49	24.33	22.52
Elongation at break/%	477.83	494.7	468.55	452.4	460.65	473.15	473.45
Tear strength/N mm ⁻¹	65.01	84.73	78.72	69.98	69.93	73.74	68.59
Hardness/Shore A	68	66	67	67	68	67	67



with sample 1# (65.01 Mpa), the corresponding values of tensile strength (25.02 MPa) and elongation at break (494.9%).

4. Conclusion

In this study, micro-spherical structure N90 and N98 is studied to effect on flex fatigue property and plasticizing behavior of NR. This result can demonstrate that addition of N90 and N98 is helpful for dispersion of carbon black. Spherical N90 and N98 are embedded in the filler–filler and filler–polymer network structure to play lubrication action which reducing the inter-molecular frictions. Then, spherical N90 and N98 can lubricate the movement of the molecules reducing their internal resistance to slide and to prevent the re-formation of the rigid matrix. This efficient slide between molecules can consume a large amount of energy. The results indicate that the slowest crack growth rate at a given tearing energy for the NR plasticized with 5 phr N90 denotes the strongest resistance to crack growth compared with the other compounds. The maximum tear strength (84.73 Mpa) is also obtained using 5 phr N90, along with the lowest tear strength, the corresponding values of tensile strength (25.02 MPa), elongation at break (494.9%).

Conflicts of interest

There are no conflicts to declare.

Acknowledgements

The authors gratefully acknowledge support from National Natural Science Foundation of China [grant numbers 51703111 and 51603111] and Shandong Provincial Natural Science Foundation, China [grant numbers 2018GGX102015 and ZR2017BEM011].

References

- 1 *Blends of Natural Rubber*, A. J. Tinker and K. P. Jones, Chapman & Hall, London, 1998.
- 2 A. Y. Coran, Blends of dissimilar rubbers-cure-rate incompatibility, *Rubber Chem. Technol.*, 1988, **61**, 281.
- 3 N. Kuhakongkiat, V. Wachteng, S. Nobukawa and M. Yamaguchi, Interphase transfer of plasticizer between immiscible rubbers, *Polymer*, 2015, **78**, 208–211.
- 4 C. Nakason, A. Kaesaman, Z. Samoh, S. Homsin and S. Kiatkamjornwong, Rheological properties of maleated natural rubber and natural rubber blends, *Polym. Test.*, 2002, **21**, 449.
- 5 U. N. Okwu and F. E. Okieimen, Preparation and properties of thioglycolic acid modified epoxidised natural rubber and its blends with natural rubber, *Eur. Polym. J.*, 2001, **37**, 2253–2258.
- 6 S. H. Goh, Characterization of natural rubber/polyisoprene rubber blends by differential scanning calorimetry, *Thermochim. Acta*, 1980, **41**, 261–264.
- 7 T. Zaharescu, V. Meltzer and R. Vilcu, Thermal properties of EPDM/NR blends, *Polym. Degrad. Stab.*, 2000, **70**, 341–345.
- 8 H. Ismail and H. C. Leong, Curing characteristics and mechanical properties of natural rubber/chloroprene rubber and epoxidized natural rubber/chloroprene rubber blends, *Polym. Test.*, 2001, **20**, 509–516.
- 9 A. J. Tinker, Crosslink distribution and interfacial adhesion in vulcanized blends of NR and NBR, *Rubber Chem. Technol.*, 1990, **63**, 503–515.
- 10 T. Y. Jiang and C. F. Zukoski, Role of particle size and polymer length in rheology of colloid-polymer composites, *Macromolecules*, 2012, **45**, 9791–9803.
- 11 W. Kim, A. Argento, C. Flanigan and D. F. Mielewski, Effects of soy-based oils on the tensile behavior of EPDM rubber, *Polym. Test.*, 2015, **46**, 33–40.
- 12 Mobil, *Developmental toxicity in rats exposed dermally to 318 isthmus furfural extract*, Mobil Environmental Health and Safety Department, 1990, Study No. 62884.
- 13 S. M. A. Doak, V. K. H. Brown, P. F. Hunt, J. D. Smith and F. J. C. Roe, The carcinogenic potential of twelve refined mineral oils following long-term topical application, *Br. J. Cancer*, 1983, **48**, 429–436.
- 14 M. S. Evans, *Tyre compounding for improved performance*, R-Report, 2001, vol. 12(8), p. 84.
- 15 M. H. Feuston, C. E. Hamilton and C. R. Mackerer, Systemic and developmental toxicity of dermally applied distillate aromatic extract in rats, *Fundam. Appl. Toxicol.*, 1996, **30**, 276.
- 16 L. Li, J. Zhang, J. O. Jo, S. Datta and J. K. Kim, Effects of variation of oil and zinc oxide type on the gas barrier and mechanical properties of chlorobutyl rubber/epoxidised natural rubber blends, *Mater. Des.*, 2013, **49**, 922–928.
- 17 N. Kuhakongkiat, V. Wachteng, S. Nobukawa and M. Yamaguchi, Interphase transfer of plasticizer between immiscible rubbers, *Polymer*, 2015, **78**, 208–211.
- 18 G. Wypych, *Handbook of Plasticizers*, Elsevier, Toronto, Canada, 2012.
- 19 L. L. P. R. Andrade and K. Rajagopal, Models for estimating the viscosity of paraffinic-naphthenic live crude oils, *Energy Fuels*, 2018, **32**(2), 2622–2629.
- 20 G. D. Feng, L. H. Hu, Y. Ma, P. Y. Jia, Y. Hu, M. Zhang, C. G. Liu and Y. H. Zhou, An efficient bio-based plasticizer for poly (vinyl chloride) from waste cooking oil and citric acid: Synthesis and evaluation in PVC films, *J. Cleaner Prod.*, 2018, **189**, 334–343.
- 21 B. Valentina, R. K. Rit, R. Kirchmann, A. Stefania Trita and L. J. Gooßen, Synthesis of bio-based surfactants from cashew nutshell liquid in water, *Green Chem.*, 2018, **20**, 3210.
- 22 S. Mohapatra and G. B. Nando, Cardanol: a green substitute for aromatic oil as a plasticizer in natural rubber, *RSC Adv.*, 2014, **4**, 15406–15418.
- 23 Z. L. Gong, L. Cen, S. T. Wang and F. L. Chen, Synthesis and characterization of maleated glycidyl 3-pentadecenyl phenyl ether as a functionalized plasticizer for styrene–butadiene rubber/carbon black/silica composites, *J. Appl. Polym. Sci.*, 2014, 40462–40469.
- 24 G. Wypych, *Handbook of plasticizers*, Chem Tec Publishing, Canada, 2004.



- 25 T. Nakazono and A. Matsumoto, Mechanical properties and thermal aging behavior of styrene-butadiene rubbers vulcanized using liquid diene polymers as the plasticizer, *J. Appl. Polym. Sci.*, 2010, **118**(4), 2314–2320.
- 26 H. L. Kang, Y. S. Li, M. Gong, Y. L. Guo, Z. Guo, Q. H. Fang and X. Li, An environmentally sustainable plasticizer toughened polylactide, *RSC Adv.*, 2018, **8**, 11643–11651.
- 27 T. Nakazono, A. Ozaki and A. Matsumoto, Phase separation and thermal aging behavior of styrene-butadiene rubber vulcanizates using liquid polymers as plasticizers studied by differential scanning calorimetry and dynamic mechanical spectroscopy, *J. Appl. Polym. Sci.*, 2011, **120**(1), 434–440.
- 28 Y. Q. Ren, S. Zhao, Q. Yao, Q. Q. Li, X. Y. Zhang and L. Q. Zhang, Effects of plasticizers on the strain-induced crystallization and mechanical properties of natural rubber and synthetic polyisoprene, *RSC Adv.*, 2015, **5**, 11317–11324.
- 29 J. J. Abraham, S. Thomas and S. C. George, Micro and nano TiO₂ reinforced natural rubber composites, *Natural Rubber Materials*, 2013, pp. 290–306.
- 30 A. P. Meera, S. Said, Y. Grohens, A. S. Luyt and S. Thomas, Tensile stress relaxation studies of TiO₂ and nanosilica filled natural rubber composites, *Ind. Eng. Chem. Res.*, 2009, **48**(7), 3410–3416.
- 31 J. Zheng, D. Han, X. Ye, X. Wu, Y. Wu, Y. Wang and L. Q. Zhang, Chemical and physical interaction between silane coupling agent with long arms and silica and its effect on silica/natural rubber composites, *Polymer*, 2018, **135**, 200–210.
- 32 S. Pattanawanidchai, S. Loykulnant, P. Sae-oui, N. Maneevas and C. Sirisinha, Development of eco-friendly coupling agent for precipitated silica filled natural rubber compounds, *Polym. Test.*, 2014, **34**, 58–63.
- 33 P. H. Daniels, A brief overview of theories of PVC plasticization and methods used to evaluate PVC-plasticizer interaction, *J. Vinyl Addit. Technol.*, 2009, **15**, 219–223.
- 34 J. E. Mark, B. Erman and F. R. Eirich, *The Science and technology of rubber*, Elsevier Academic, San Diego, CA, 2005.
- 35 W. J. Zheng, X. J. Gao, Y. Liu, L. M. Wang, J. G. Yang and Z. L. Gao, Industrial Mooney viscosity prediction using fast semi-supervised empirical model, *Chemom. Intell. Lab. Syst.*, 2017, **171**, 86–92.
- 36 E. K. Hobbie, T. Ihle, J. M. Harris and M. R. Semler, Empirical evaluation of attractive van der waals potentials for type-purified single-wall carbon nanotubes, *Phys. Rev. B: Condens. Matter Mater. Phys.*, 2012, **85**, 245439.
- 37 E. R. Smith, D. J. Mitchell and B. W. Ninham, Deviations of the van der waals energy for two interacting spheres from the predictions of Hamaker theory, *J. Colloid Interface Sci.*, 1973, **45**, 55–56.
- 38 N. Rattanasoma, T. Saowapark and C. Deeprasertku, Reinforcement of natural rubber with silica/carbon black hybrid filler, *Polym. Test.*, 2007, **26**, 369–377.
- 39 J. Fröhlich, W. Niedermeier and H. D. Luginsland, The effect of filler-filler and filler-elastomer interaction on rubber reinforcement, *Composites, Part A*, 2005, **36**, 449–460.
- 40 E. F. Miroslawa, P. Prowans, J. E. Puskas and V. Altstadt, Biocompatibility and fatigue properties of polystyrene-polyisobutylene-polystyrene, an emerging thermoplastic elastomeric biomaterial, *Biomacromolecules*, 2006, **7**, 844–850.

